Am J Transl Res 2020;12(12):7762-7781
www.ajtr.org /ISSN:1943-8141/AJTR0114082

*Original Article*

# Ahypoxia-related signature enhances the prediction of the prognosis in hepatocellular carcinoma patients and correlates with sorafenib treatment response

Hong-Ye Jiang[1], Gang Ning[2], Yen-Sheng Wang[3], Wei-Biao Lv[1]

*[1]Department of Clinical Laboratory, Shunde Hospital, Southern Medical University (The First People's Hospital of Shunde), Foshan 528308, Guangdong Province, PR China; [2]Department of Gastroenterology and Hepatology, Guangzhou Digestive Diseases Center, Guangzhou First People's Hospital, South China University of Technology, Guangzhou, Guangdong Province, PR China; [3]Department of Medicine, Chang-Gung Memorial Hospital, Linkou, Taiwan, PR China*

Received May 9, 2020; Accepted October 24, 2020; Epub December 15, 2020; Published December 30, 2020

**Abstract:** Hepatocellular carcinoma (HCC) is one of the leading cancer death and is the primary malignancy of the liver. Tumor hypoxia is the stressor that is involved in tumorigenesis and significantly increased the aggressiveness of HCC. Here, we systematically analyzed the expression profiles and prognostic values of 84 hypoxia associated genes in HCC. mRNA expression of 84 hypoxia associated genes and clinical parameters of HCC patients were downloaded from TCGA, GSE14520, GSE109211 and ICGC. Consensus clustering analysis was performed for unsupervised classes on the basis of 84 hypoxia associated genes. Univariate and LASSO analysis were used to develop the risk signature. A risk signature was developed, including the expression of APEX1, ATR, CTSA, DNAJC5, ENO1, EPO, HMOX1, LDHA, NDRG1, and PER1, and found to be significantly related with OS and DFS of HCC patients. We stratified HCC patients into the high-risk group and low-risk group by means of the risk signature. Patients of high-risk group had shorter OS and DFS, while that of the low-risk group had longer OS and DFS. The risk signature showed better predictive efficiency than the TNM staging in predicting OS and DFS. Also, macrophage M0 cells, regulatory T cells, and neutrophils were found to be significantly enriched in patients of high-risk group. Next, we validated the discrimination and prognostic value of the risk signature in GSE14520 and the ICGC HCC cohort. Finally, significantly lower risk scores were found in sorafenib treatment responders of GSE109211 cohort, and the AUC for predicting sorafenib treatment response was 0.881. In conclusion, a risk signature developed with the expression of 10 hypoxia associated genes improved the prognosis prediction of HCC and correlated with sorafenib treatment response.

**Keywords:** Hypoxia, HCC, risk signature, prognosis, sorafenib, treatment response

## Introduction

Hepatocellular carcinoma (HCC) is one of the leading cancer death and is the primary malignancy of the liver. During 2018, nearly 841,000 patients developed HCC and 782,000 patients died of HCC [1]. Moreover, in areas with low historical rates, including Oceania, and Western Europe, the incidence of HCC is increasing rapidly [2]. Despite there being many options for the treatment of HCC, such as hepatectomy, liver transplantation, thermal or chemical ablation, trans-arterial chemoembolization, radiation and chemotherapy [3, 4], none of them are amenable curative therapies, as HCC behaves highly refractory to most of them. For example, more than 50% of patients will relapse after resection, which renders the 5-year survival rate < 30% [5]. Therefore, exploring new efficient methods for early diagnosis and prognosis may be another important way to improve the prognosis of HCC.

Tumor hypoxia is increasingly considered as a major unfavorable factor in cancer treatment, as it could compromise anti-cancer treatment and drive malignant progression. HCC is one of the most hypoxic tumors, because the rapid proliferation of tumor cells consumes much oxygen, resulting in a hypoxic microenvironment [6]. Accumulating studies indicate that hypoxia signaling pathway is involved extensively in the

**Table 1.** Basic clinical information of 365 HCC patients from TCGA

| Variables | HCC patients (N = 365) |
|---|---|
| Gender (Male/female) | 246/119 |
| Age (years, ≤60/>60) | 173/192 |
| histologic grade (G1/G2/G3/G4) | 55/180/118/12 |
| surgical margin status (R0/R1+RX) | 327/38 |
| pathologic T stage (T1/T2/T3/T4) | 180/94/78/13 |
| pathologic N stage (N0/N1+NX) | 248/117 |
| pathologic M stage (M0/M1+MX) | 263/102 |
| pathologic stage (Stage I/II/III/IV) | 107/108/83/4 |
| vascular invasion (Macro/Micro/None) | 16/144/205 |

tumorigenesis and aggressiveness of HCC [7]. Hypoxia could promote proliferation; stimulate angiogenesis; inhibit differentiation and apoptosis; and accelerate migration, invasion and metastasis of HCC [8-10]. Moreover, hypoxia could also enhance the chemoresistance, radioresistance and resistance of trans-arterial embolization with or without chemotherapy [9, 11, 12].

Hypoxia induced factor-1 (HIF-1) is the main component of the hypoxia signaling pathway that have been studied. However, little data are available on the role of the entire subset of hypoxia signaling pathway related genes in HCC carcinogenesis. In this study, we systematically analyzed the expression pattern of 84 hypoxia associated genes and their associations with prognosis in 365 HCC patients downloaded from The Cancer Genome Atlas (TCGA). In addition, we also performed consensus clustering for unsupervised clusters of HCC patients basing on 84 hypoxia associated genes. Moreover, we developed and validated a risk signature with 10 selected genes and analyzed its prognostic value in TCGA HCC cohort, GSE14520 cohort and LIRI-JP HCC cohort of the International Cancer Genome Consortium (ICGC). Finally, the prediction values of the risk signature in sorafenib treatment response were also evaluated in the GSE109211 cohort.

## Materials and methods

### *Ethics statement*

All the data used for analysis were obtained from dataset of TCGA, Gene Expression Omnibus (GEO) dataset or ICGC. Informed consents were given to the patient and were later obtained before the study.

### *Hypoxia signaling pathway related genes*

In the present study, we carefully selected 84 hypoxia associated genes based on a thorough literature review, which has shown to have close pathway correlation mainly involved in the response to hypoxia and oxidative stress. The physiological processes induced by hypoxia associated genes were screened referring to ExProfileTM Human Hypoxia Signaling Related Gene, which was used to profile human genes related to hypoxia signaling (Supplementary Materials).

### *Data acquirement of TCGA, GEO and ICGC*

RNA sequencing data (UNC IlluminaHiSeq_RNASeqV2; Level 3) of 374 HCC patients and 50 healthy controls were attained from TCGA (https://cancergenome.nih.gov/). Meanwhile, corresponding clinical-pathological data, including gender, age, histologic grade, surgical margin status, pathologic T, N and M stage, TNM stage, vascular invasion, overall survival (OS) and disease-free survival (DFS). 9 out of 374 patients were removed due to lack of information of OS (or the OS time was zero), therefore, mRNA expression of 365 HCC and their clinical-pathologic data were used for analysis. We used following method to deal with the missing values. The R impute package was used to impute the missing data [13]. The basic clinical characteristics of the 365 patients were presented in **Table 1**.

Gene expression profiles of GSE14520 and GSE109211 were attained from GEO database (https://www.ncbi.nlm.nih.gov/geo/). In GSE14-520, the OS and DFS information of 220 HCC patients were available [14]. In GSE109211, there were 21 sorafenib treatment responders and 46 nonresponders. Moreover, a total of 230 HCC patients with available OS information and mRNA expression profile were also attained from LIRI-JP HCC cohort of ICGC portal (https://dcc.icgc.org) [15].

### *Consensus clustering analysis*

Consensus clustering is often used for unsupervised class discovery in genomic studies. We performed consensus clustering analysis for unsupervised classes of HCC patients

based on expression similarity of hypoxia associated genes with ConsensusClusterPlus packages.

*Development and validation of risk signature*

First, univariate Cox analysis was used to identify prognosis-related hypoxia associated genes. Next, we used least absolute shrinkage and selection operator (LASSO) analysis to further select those most significant prognosis-related genes [16]. Moreover, GSE14520 cohort and LIRI-JP cohort were used to independently test the applicability of the risk signature.

*Gene set enrichment analysis (GSEA)*

To explore the mechanism exploited by Cluster status or risk signature in hepato-carcinogenesis, GSEA was performed to find the different KEGG pathways between HCC patients with different Cluster status or HCC patients of different risk groups [17]. We referenced the annotated gene set (msigdb.v6.2.symbols.gmt) in our analysis.

*Cibersort*

We calculated the proportion of 22 kinds of tumor-infiltrating immune cells basing on transcriptomic data of HCC patients through Cibersort (https://cibersort.stanford.edu) [18]. Linear support vector regression was used to deconvolve the relative fractions of immune cells from the transcriptional profiles of a sample on the basis of a referenced signature matrix.

*Statistical analysis*

We used R software (R version 3.5.1) for performance of statistical analysis. The Wilcox test was performed to compare the difference of tumor-infiltrating immune cells between patients with different risk score or distinct Cluster status or the expression difference of 84 hypoxia associated genes between HCC patients and healthy controls. The association of clinical-pathologic parameters with the Cluster status was analyzed by chi-square test. The prognostic value of Cluster status or the risk signature was assessed by univariate and multivariate Cox analysis, and Kaplan-Meier analysis was conducted to analyze the difference of OS or DFS. Time-dependent ROC was performed to analyze the predictive accuracy and sensitivity of risk signature, and the area under the ROC curve (AUC) was also calculated. Additional statistical analyses were conducted with STAMP [19]. We defined $P < 0.05$ as statistically significant.

## Results

*Expression of hypoxia associated genes in HCC patients*

mRNA expression of 84 hypoxia associated genes of 365 HCC patients and 50 healthy controls were download from TCGA. As is shown in **Figure 1**, 51 out of 84 genes, including HNF4A, NCOA1, TPI1, P4HB, USF2, MET, EIF4EBP1, ENO1, PFKL, VDAC1, TP53, PGK1, ARNT, ODC1, APEX1, GPI, DDIT4, EGLN1, ERO1A, VEGFA, MIF, RUVBL2, RBPJ, ALDOA, CTSA, MAP3K1, LGALS3, NDRG1, COPS5, GYS1, ANXA2, DNAJC5, JMJD6, CCNG2, CA9, EGLN2, TFRC, PDK1, ATR, PKM, HIF1AN, SLC2A1, ADORA2B, PFKP, PLAU, PGF, SLC16A3, MMP9, LOX, PFKFB4 and BLM, were found to be overexpressed in HCC patients, while significantly higher expression of 17 genes, including FOS, EPO, EGR1, SERPINE1, IGFBP3, F3, NAMPT, HMOX1, ADM, PFKFB3, ANKRD37, SLC2A3, BHLHE40, PER1, ANGPTL4, TXNIP and LDHA, were found in normal healthy controls (all $P < 0.05$).

*Two clusters of HCC patients identified by consensus clustering basing on hypoxia associated genes expression*

Consensus clustering analysis was performed for discovery of unsupervised classes of HCC patients basing on hypoxia associated genes expression. 365 HCC patients were classified to two distinct clusters with different clinical parameters and prognosis (**Figure 2A**). As is shown in **Table 2**, we also explored the associations between Cluster status and clinical characteristics. Statistically significant differences in histologic grade, surgical margin status, pathologic T stage, pathologic stage and vascular invasion were found between Cluster 1 (n = 245) and Cluster 2 (n = 120). There were significantly more patients with advanced histologic grade, pathologic T stage and pathologic stage or patients with positive margin status and vas-

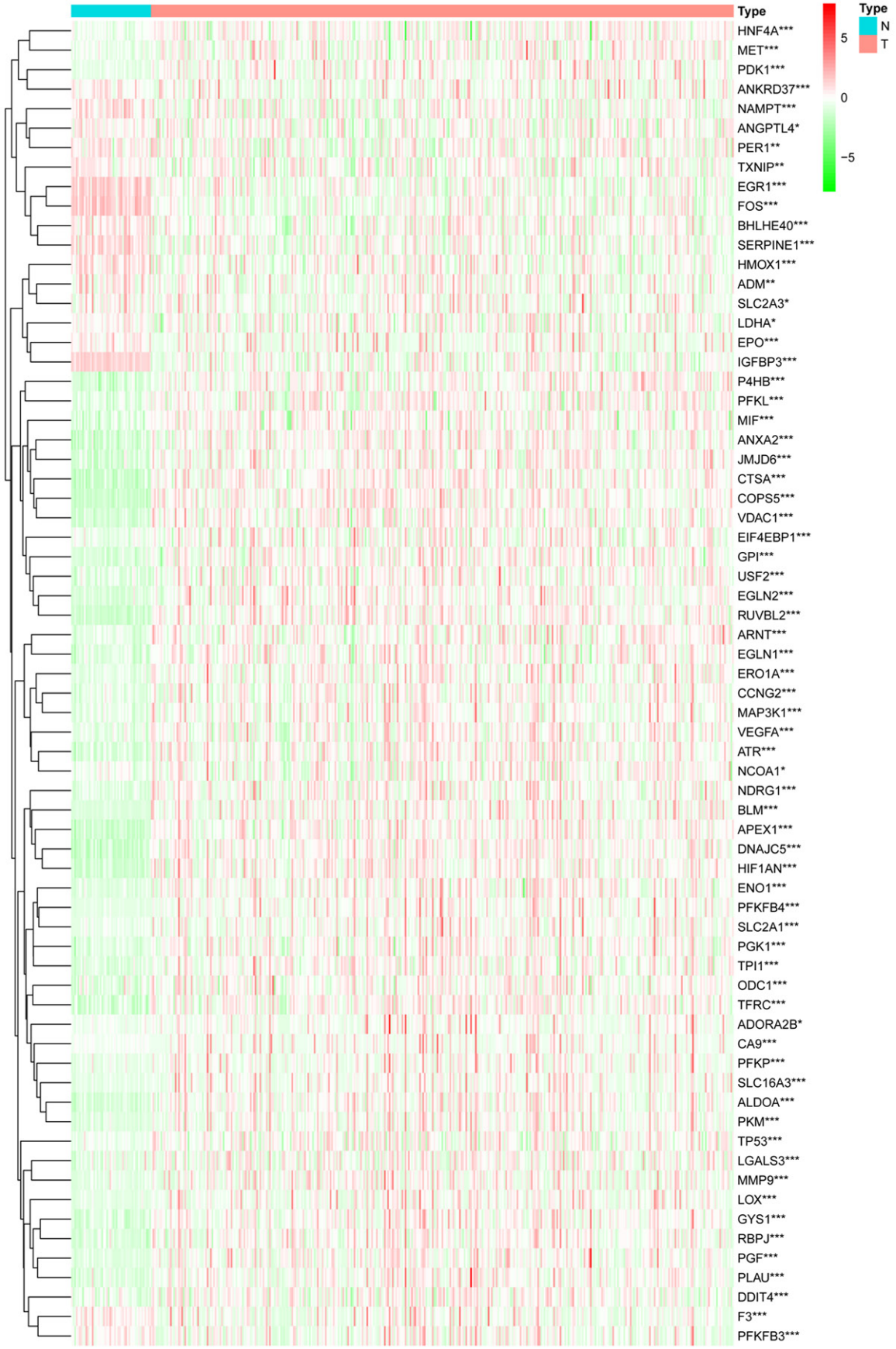
Type
HNF4A***
MET***
PDK1***
ANKRD37***
NAMPT***
ANGPTL4*
PER1**
TXNIP**
EGR1***
FOS***
BHLHE40***
SERPINE1***
HMOX1***
ADM**
SLC2A3*
LDHA*
EPO***
IGFBP3***
P4HB***
PFKL***
MIF***
ANXA2***
JMJD6***
CTSA***
COPS5***
VDAC1***
EIF4EBP1***
GPI***
USF2***
EGLN2***
RUVBL2***
ARNT***
EGLN1***
ERO1A***
CCNG2***
MAP3K1***
VEGFA***
ATR***
NCOA1*
NDRG1***
BLM***
APEX1***
DNAJC5***
HIF1AN***
ENO1***
PFKFB4***
SLC2A1***
PGK1***
TPI1***
ODC1***
TFRC***
ADORA2B*
CA9***
PFKP***
SLC16A3***
ALDOA***
PKM***
TP53***
LGALS3***
MMP9***
LOX***
GYS1***
RBPJ***
PGF***
PLAU***
DDIT4***
F3***
PFKFB3***
Type
N
T
5
0
−5

**Figure 1.** Heatmap of log2 expression of 84 hypoxia signaling pathway related genes between HCC patients and normal controls in the TCGA HCC cohort, and there were 51 over-expressed genes and 17 down-regulated genes in HCC. N: normal, T: tumor; *P < 0.05, **P < 0.01, ***P < 0.001.

A

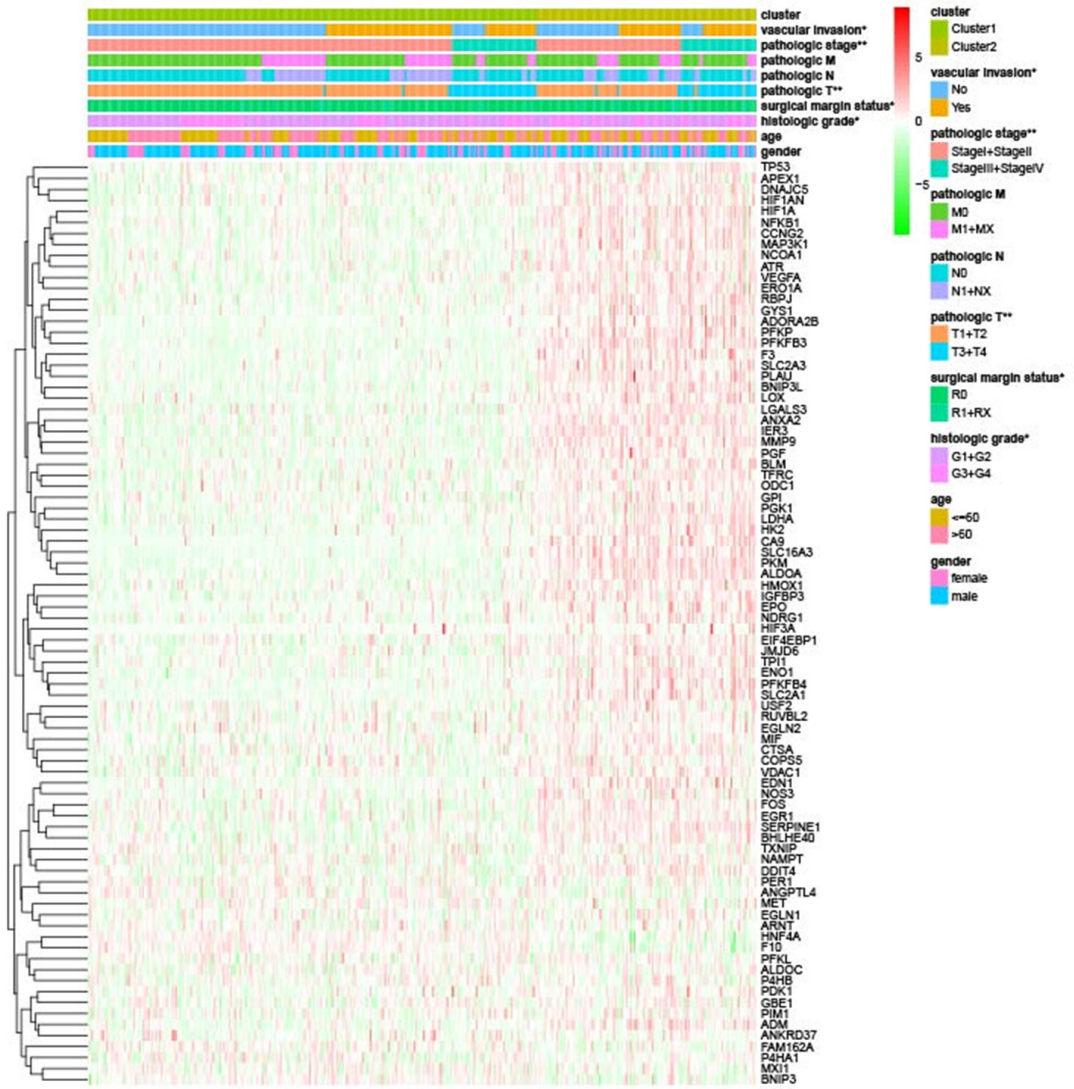

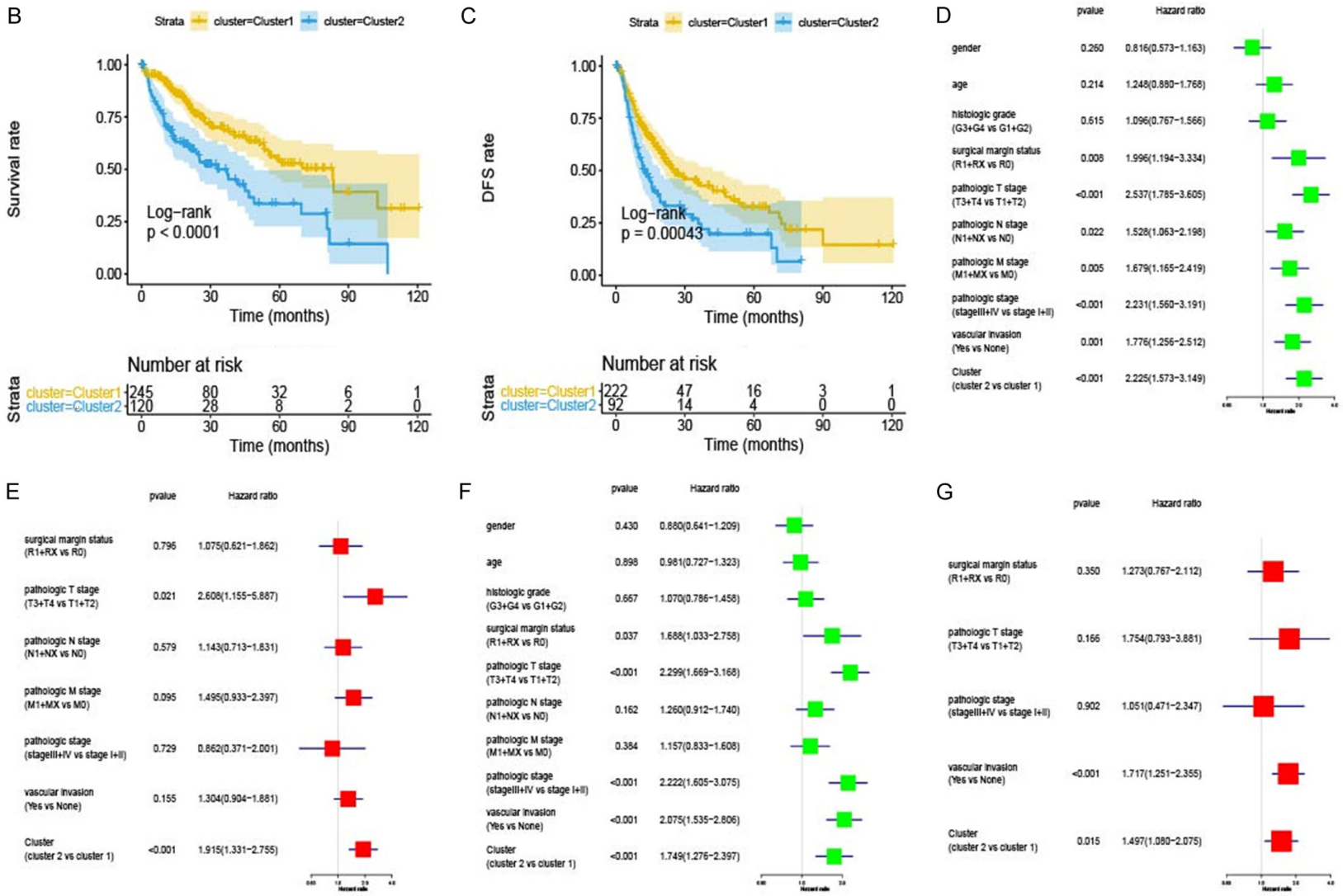


**Figure 2.** Two clusters of HCC patients identified by consensus clustering of 84 hypoxia associated genes in the TCGA cohort. A. Heatmap of the association of clinical-pathologic parameters with Cluster status, there were significantly more patients with advanced histologic grade, pathologic T stage and pathologic stage or patients with positive margin status and vascular invasion in Cluster 2. B, C. Kaplan-Meier analysis of OS and DFS of patients from the two clusters, and patients of Cluster 1 had longer OS and DFS. D-G. Univariate and multivariate analysis of Cluster status, the cluster status was independently associated with prognosis of OS and DFS. OS: overall survival; DFS: disease-free survival.

**Table 2.** Demographic and clinical characteristics of HCC patients of different clusters

| Variables | Cluster 1 | Cluster 2 | *p*-value |
|---|---|---|---|
| Number of patients | 245 | 120 | |
| Gender (Male/female) | 172/73 | 74/46 | 0.13 |
| Age (years, ≤60/>60) | 114/131 | 59/61 | 0.72 |
| histologic grade (G1+G2/G3+G4) | 168/77 | 67/53 | 0.02 |
| surgical margin status (R0/R1+RX) | 227/18 | 100/20 | 0.01 |
| pathologic T stage (T1/T2/T3/T4) | 196/49 | 78/42 | 0.003 |
| pathologic N stage (N0/N1+NX) | 166/79 | 78/42 | 0.99 |
| pathologic M stage (M0/M1+MX) | 174/71 | 89/31 | 0.61 |
| pathologic stage (Stage I+II/Stage III+IV) | 199/46 | 79/41 | 0.002 |
| vascular invasion (Yes/None) | 97/148 | 53/57 | 0.03 |

cular invasion in Cluster 2 (all P < 0.05). In addition, patients in Cluster 1 had longer OS (median OS time: 83.18 vs 33.02 months, HR = 0.4, 95% CI: 0.27-0.59, P < 0.001) and longer DFS (median DFS time: 25.3 vs 12.68 months, HR = 0.58, 95% CI: 0.37-0.75, P < 0.001) compared to patients in Cluster 2 (**Figure 2B**, **2C**). Moreover, Cluster status was significantly related with OS and DFS, and it was also an independent prognostic factor for OS and DFS in HCC patients suggesting by univariate and multivariate Cox analysis (all P < 0.001, **Figure 2D-G**).

*Potential mechanism by which Cluster status influenced prognosis and the landscape of tumor-infiltrating immune cells in patients with different Cluster status*

We performed GSEA of 365 HCC patients with different Cluster status to explore the underlying biological mechanism by which Cluster status influenced prognosis. As is shown at **Figure 3A**, KEGG pathways, such as "Cell cycle", "Pathways in cancer", "P53 signaling pathway", "TGF-β signaling pathway", "WNT signaling pathway" and "MAPK signaling pathway" were significantly enriched in patients of Cluster 2 compared to patients of Cluster 1, suggesting that the aforementioned biological process played an important role in Cluster status influencing prognosis.

Moreover, differences in the proportions of different tumor-infiltrating immune cells between patients with different Cluster status are also analyzed. As is shown at **Figure 3B**, in general, patients in Cluster 1 seemed to have higher immune infiltration of T and B cells. Significantly higher proportions of resting mast cells, resting NK cells, monocytes, resting CD4 memory cells, naive B cells and naive CD4 T cells were found in patients of Cluster 1 (all P < 0.05), while significantly higher proportions of macrophage M0 cells, activated CD4 memory cells, neutrophils, plasma cells and memory B cells were found in patients of Cluster 2 (all P < 0.05). These results suggested that different kinds of tumor-infiltrating immune cells in patients with different Cluster status may contribute to their different prognosis.

*Development of a risk signature with 10 hypoxia associated genes and its prognostic value*

To better explore the prognostic value of hypoxia associated genes, we developed a risk signature. First, we performed univariate analysis to identify OS-related genes. As is shown in **Table 3**, there were 41 hypoxia associated genes to be significantly related to OS. Next, LASSO analysis was performed to further select the most significant OS-related genes. A total of 10 genes, including APEX1, ATR, CTSA, DNAJC5, ENO1, EPO, HMOX1, LDHA, NDRG1 and PER1, were identified according to the minimum criteria (**Figure 4A**, **4B**). A risk signature was built based on the coefficients weighted by LASSO analysis and calculated as follows: risk score = (0.005*APEX1 expression) + (0.0002*ATR expression) + (0.003*CTSA expression) + (0.001*DNAJC5 expression) + (0.0002*ENO1 expression) + (0.003*EPO expression) + (0.001*HMOX1 expression) + (0.004* LDHA expression) + (0.004*NDRG1 expression) - (0.006*PER1 expression). We calculated risk score for each patient, and 365 patients were divided into a high risk subgroup and a low risk subgroup based on the median risk score. We noticed that patients in the high risk subgroup had poorer OS (median OS time: 37.29 vs 102.7 months, HR = 2.57, 95% CI: 1.81-3.65, P < 0.001, **Figure 4C**) and shorter DFS (median DFS: 13.63 vs 35.58 months, HR = 1.90, 95% CI: 1.40-2.58, P < 0.001, **Figure 4D**) compared to patients in the low risk subgroup. Moreover,

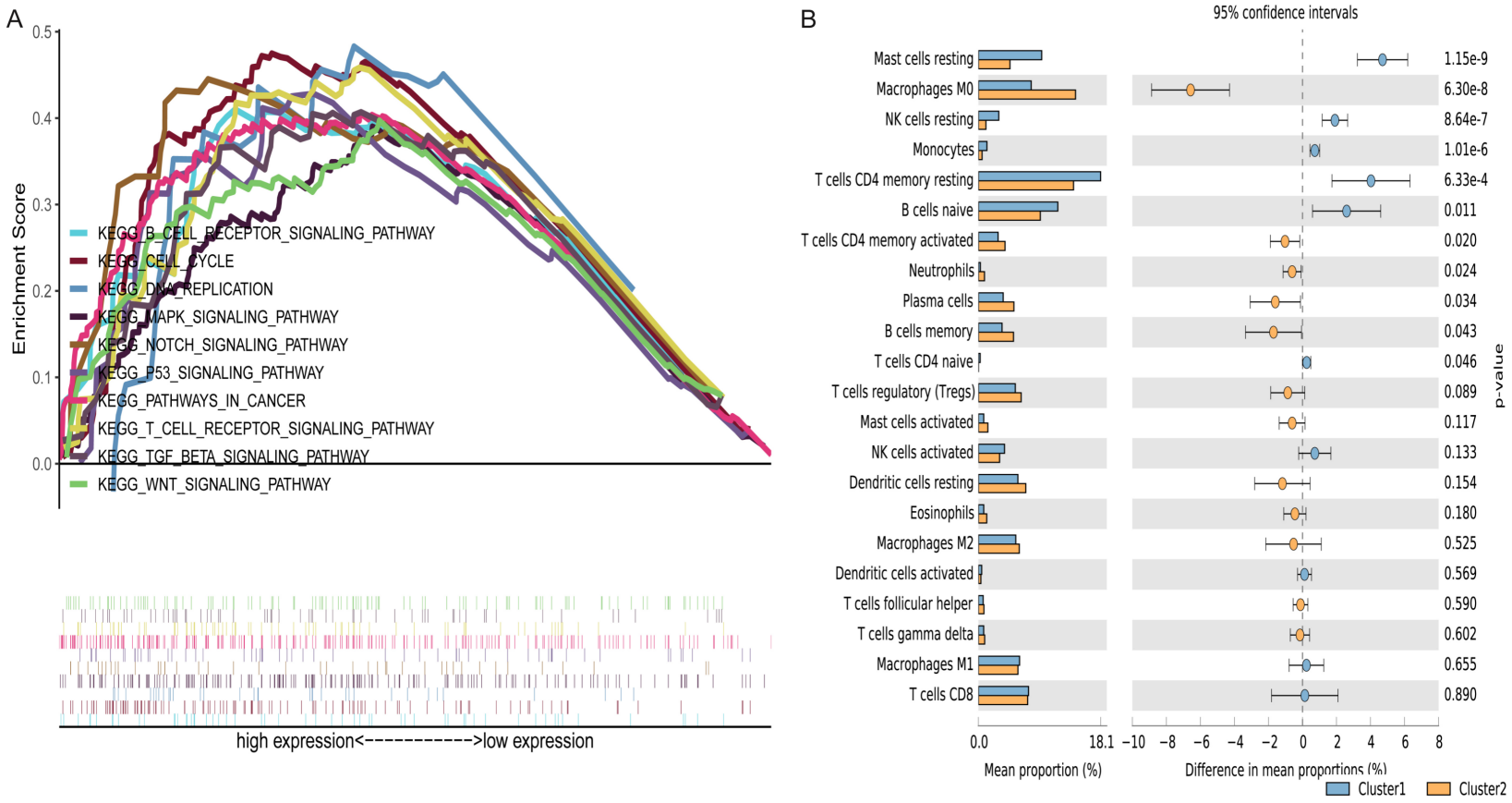


**Figure 3.** Potential mechanism by which Cluster status influenced prognosis and the landscape of tumor-infiltrating immune cells in patients with different Cluster status. A. Gene set enrichment analysis of in patients with different Cluster status in the TCGA HCC cohort, KEGG pathways, such as "*P53* signaling pathway", "TGF-β signaling pathway", "WNT signaling pathway" were significantly enriched in patients of Cluster 2; B. Landscape of tumor-infiltrating immune cells in patients with different Cluster status in the TCGA cohort, patients in Cluster 1 had higher immune infiltration than that in Cluster 2.

**Table 3.** Prognosis associated hypoxia signaling pathway related genes identified by univariate Cox analysis

| Gene | HR | 95% CI (low) | 95% CI (high) | *P* value |
|---|---|---|---|---|
| ENO1 | 1.002 | 1.001 | 1.003 | 1.99E-08 |
| LDHA | 1.009 | 1.006 | 1.012 | 1.48E-07 |
| NDRG1 | 1.007 | 1.005 | 1.010 | 2.70E-07 |
| PFKFB4 | 1.263 | 1.151 | 1.386 | 8.83E-07 |
| SLC2A1 | 1.062 | 1.035 | 1.089 | 4.55E-06 |
| CTSA | 1.011 | 1.006 | 1.016 | 3.04E-05 |
| EPO | 1.033 | 1.017 | 1.049 | 5.87E-05 |
| SLC16A3 | 1.049 | 1.024 | 1.074 | 9.13E-05 |
| APEX1 | 1.013 | 1.006 | 1.020 | 0.0001 |
| DNAJC5 | 1.049 | 1.023 | 1.076 | 0.0002 |
| JMJD6 | 1.116 | 1.050 | 1.186 | 0.0004 |
| ANXA2 | 1.007 | 1.003 | 1.011 | 0.0005 |
| HMOX1 | 1.003 | 1.001 | 1.004 | 0.0005 |
| HK2 | 1.054 | 1.023 | 1.086 | 0.001 |
| LOX | 1.066 | 1.026 | 1.108 | 0.001 |
| PGK1 | 1.005 | 1.002 | 1.008 | 0.001 |
| RUVBL2 | 1.025 | 1.010 | 1.040 | 0.001 |
| VDAC1 | 1.009 | 1.003 | 1.015 | 0.002 |
| HIF1A | 1.013 | 1.004 | 1.021 | 0.003 |
| BLM | 1.510 | 1.155 | 1.975 | 0.003 |
| ALDOA | 1.003 | 1.001 | 1.004 | 0.003 |
| VEGFA | 1.027 | 1.009 | 1.045 | 0.004 |
| TPI1 | 1.003 | 1.001 | 1.004 | 0.004 |
| PER1 | 0.953 | 0.921 | 0.985 | 0.005 |
| BNIP3L | 1.033 | 1.010 | 1.057 | 0.005 |
| ATR | 1.435 | 1.111 | 1.854 | 0.006 |
| LGALS3 | 1.007 | 1.002 | 1.011 | 0.006 |
| HIF1AN | 1.238 | 1.061 | 1.445 | 0.007 |
| ADORA2B | 1.178 | 1.043 | 1.329 | 0.008 |
| PFKFB3 | 1.010 | 1.002 | 1.018 | 0.010 |
| COPS5 | 1.064 | 1.014 | 1.116 | 0.012 |
| RBPJ | 1.121 | 1.025 | 1.227 | 0.013 |
| MAP3K1 | 1.079 | 1.011 | 1.152 | 0.022 |
| PKM | 1.003 | 1.000 | 1.006 | 0.023 |
| SERPINE1 | 1.002 | 1.000 | 1.004 | 0.024 |
| TFRC | 1.019 | 1.002 | 1.037 | 0.031 |
| PFKP | 1.009 | 1.001 | 1.017 | 0.034 |
| TXNIP | 0.997 | 0.994 | 1.000 | 0.040 |
| MMP9 | 1.004 | 1.000 | 1.008 | 0.046 |
| CCNG2 | 1.129 | 1.001 | 1.272 | 0.047 |
| NCOA1 | 1.083 | 1.000 | 1.172 | 0.049 |

the risk signature was also significantly related to OS and DFS, and it was an independent prognostic factor for OS and DFS in HCC patients (all P < 0.001) (**Figure 4E-H**).

Then, we performed time-dependent ROC curve analysis to explore the predictive value of the risk signature. As is shown at **Figure 5**, the AUC of the risk signature for predicting 1-, 3- and 5-OS were 0.76, 0.71 and 0.70, respectively (**Figure 5A**), showing better predictive efficiency compared to pathologic TNM stage, pathologic T stage and pathologic M stage (**Figure 5B**), which were all independently associated with prognosis of HCC (**Figure 4F**). Similarly, the AUC of the risk signature for predicting 1-year, 3-year and 5-year DFS were 0.68, 0.64 and 0.58, respectively (**Figure 5C**), still showing better predictive accuracy than pathologic TNM stage and vascular invasion (**Figure 5D**), which were also independent prognostic factors for DFS (**Figure 4H**).

*Potential biological KEGG pathways of the risk signature and landscape of tumor-infiltrating immune cells in different risk groups*

GSEA was also used to analyze the potential biological KEGG pathways revealed by the risk signature. As is presented in **Figure 6A**, KEGG pathways, such as “Cell cycle”, “Pyrimidine metabolism” and “Purine metabolism” were significantly enriched in patients of the high risk group compared to that in the low risk group. Besides, the differences of tumor-infiltrating immune cells between patients with different risk scores were also analyze. As is summarized in **Figure 6B**, macrophage M0 cells, regulatory T cells, and neutrophils were found to be enriched in patients with high-risk score (all P < 0.05), while resting mast cells, resting CD4 memory cells, macrophage M1 cells and monocytes were found to be enriched in patients with low risk score (all P < 0.05).

*Validation of the risk signature in the GSE14520 cohort and LIRI-JP cohort*

Further, we also independently examined the robustness of the risk signature in the GSE14520 cohort and LIRI-JP cohort, which included 220 HCC patients and 232 HCC patients, respectively. We calculated risk score for all HCC patients. Similarly, HCC patients were also assigned into two distinct subgroups with the cut-off value of median risk score. In GSE14520 cohort, patients with high risk score

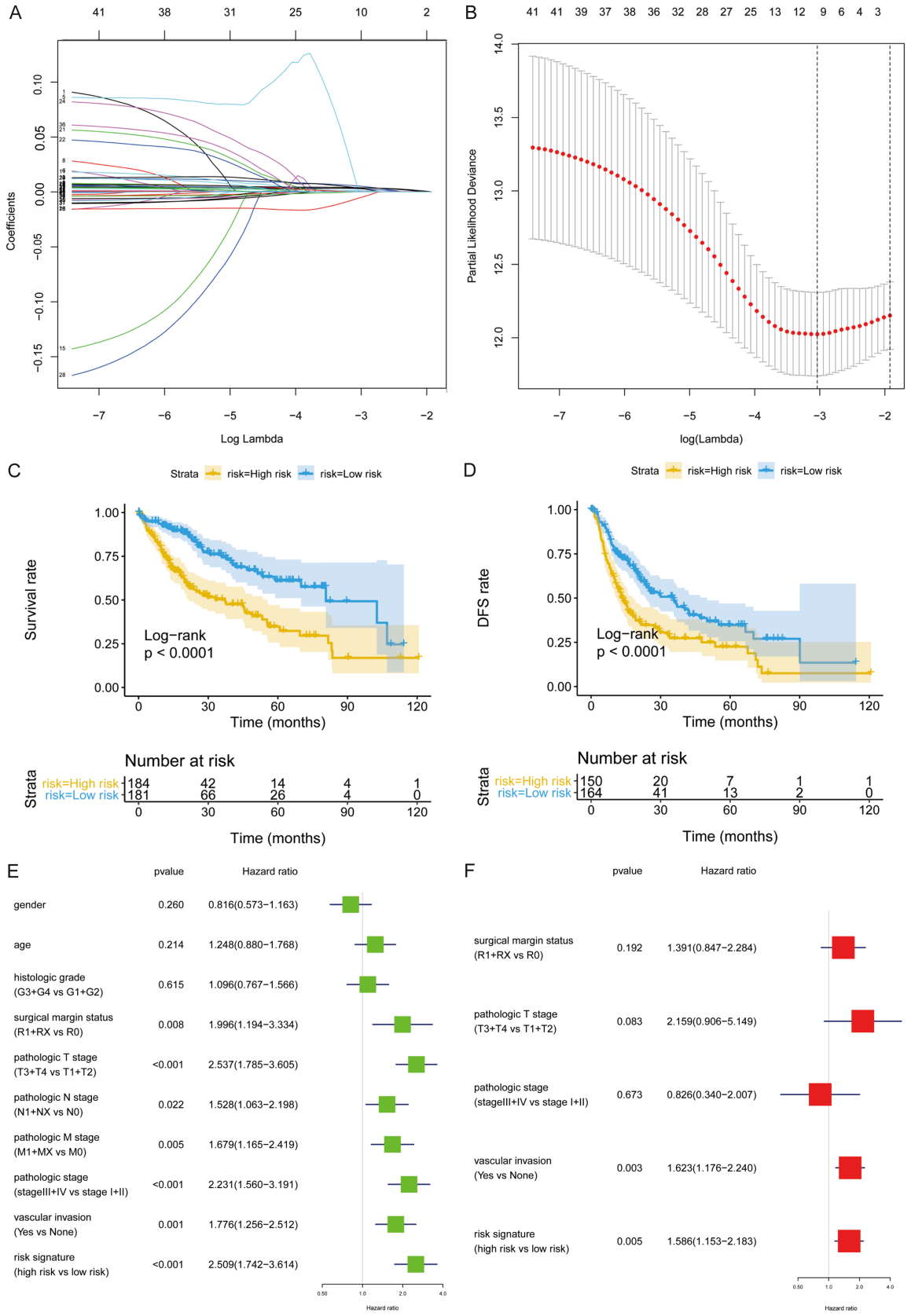
A
Coefficients
Log Lambda
B
Partial Likelihood Deviance
log(Lambda)
C
Strata risk=High risk risk=Low risk
Survival rate
Log−rank p < 0.0001
Time (months)
Number at risk
risk=High risk 184 42 14 4 1
risk=Low risk 181 66 26 4 0
D
DFS rate
Log−rank p < 0.0001
Time (months)
Number at risk
risk=High risk 150 20 7 1 1
risk=Low risk 164 41 13 2 0
E
pvalue
Hazard ratio
gender 0.260 0.816(0.573−1.163)
age 0.214 1.248(0.880−1.768)
histologic grade (G3+G4 vs G1+G2) 0.615 1.096(0.767−1.566)
surgical margin status (R1+RX vs R0) 0.008 1.996(1.194−3.334)
pathologic T stage (T3+T4 vs T1+T2) <0.001 2.537(1.785−3.605)
pathologic N stage (N1+NX vs N0) 0.022 1.528(1.063−2.198)
pathologic M stage (M1+MX vs M0) 0.005 1.679(1.165−2.419)
pathologic stage (stageIII+IV vs stage I+II) <0.001 2.231(1.560−3.191)
vascular invasion (Yes vs None) 0.001 1.776(1.256−2.512)
risk signature (high risk vs low risk) <0.001 2.509(1.742−3.614)
Hazard ratio
F
pvalue
Hazard ratio
surgical margin status (R1+RX vs R0) 0.192 1.391(0.847−2.284)
pathologic T stage (T3+T4 vs T1+T2) 0.083 2.159(0.906−5.149)
pathologic stage (stageIII+IV vs stage I+II) 0.673 0.826(0.340−2.007)
vascular invasion (Yes vs None) 0.003 1.623(1.176−2.240)
risk signature (high risk vs low risk) 0.005 1.586(1.153−2.183)
Hazard ratio

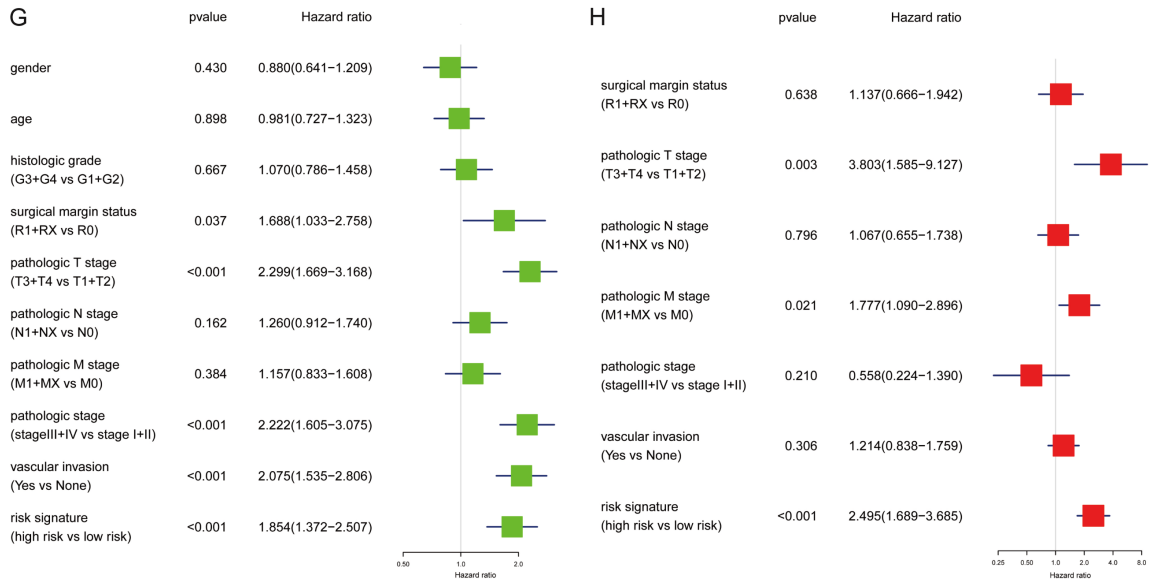


**Figure 4.** Development of risk signature with 10 hypoxia signaling pathway related genes and its association with prognosis of HCC patients in the TCGA cohort. A, B. A total of 10 hypoxia associated genes were identifed to be signifcantly related to OS by LASSO analysis. C, D. Kaplan-Meier analysis of OS and DFS of patients with different risk scores, and patients in the high risk subgroup had poorer OS and shorter DFS. E-H. Univariate and multivariate analysis of risk signature for OS and DFS, the risk signature was independently associated with prognosis of OS and DFS.

had poorer OS (HR = 2.66, 95% CI: 1.73-4.11, P < 0.001, **Figure 7A**) and shorter DFS (HR = 1.63, 95% CI: 1.14-2.34, P < 0.001, **Figure 7B**) than patients with low risk score. The 1-, 3- and 5-year OS predicted by the risk signature were 0.66, 0.68 and 0.69, respectively (**Figure 7C**), and 1-, 3- and 5-year DFS predicted by the risk signature were 0.65, 0.63 and 0.62, respectively (**Figure 7E**). In LIRI-JP cohort, the signature could also effectively stratify HCC patients into high risk subgroup with poorer OS and low risk subgroup with better OS (HR=3.86, 95% CI: 2.04-6.82, P < 0.001, **Figure 7D**). The 1-, 3- and 5-year OS predicted by the risk signature were 0.80, 0.75 and 0.76, respectively (**Figure 7F**). Taken together, these results convincingly demonstrated the robust performance of our signature in different distinct cohorts.

*Risk signature as treatment response indicator in HCC patients with sorafenib treatment*

To explore the relationship of risk signature with the sorafenib treatment response, we also calculated risk score for 67 HCC patients with sorafenib treatment downloaded from GSE-109211, which included 21 sorafenib treatment responders and 46 nonresponders. Our results showed that significantly higher risk scores were found in sorafenib treatment non-responders compared to responders (P < 0.001, **Figure 8A**). In addition, the AUC for predicting sorafenib treatment response was 0.881 (**Figure 8B**). Taken together, the risk signature may be used as a treatment response indicator for HCC patients treated with sorafenib.

## Discussion

Tumor hypoxia is considered a major unfavorable factor in cancer treatment [7]. HCC is one of the most hypoxic tumors, and the hypoxia signaling pathway seems to be functionally relevant and therapeutically targetable in HCC. The pathway has been shown to be involved extensively in the growth and transformation of HCC and compromises anti-cancer treatment by regulation of proliferation, angiogenesis, differentiation, apoptosis and metastasis [7-10]. Despite the relationship between some hypoxia associated genes and HCC having been explored in previous studies [20-22], in-depth analysis of all hypoxia associated genes in HCC has not been performed. Moreover, the prognostic value of the total hypoxia associated

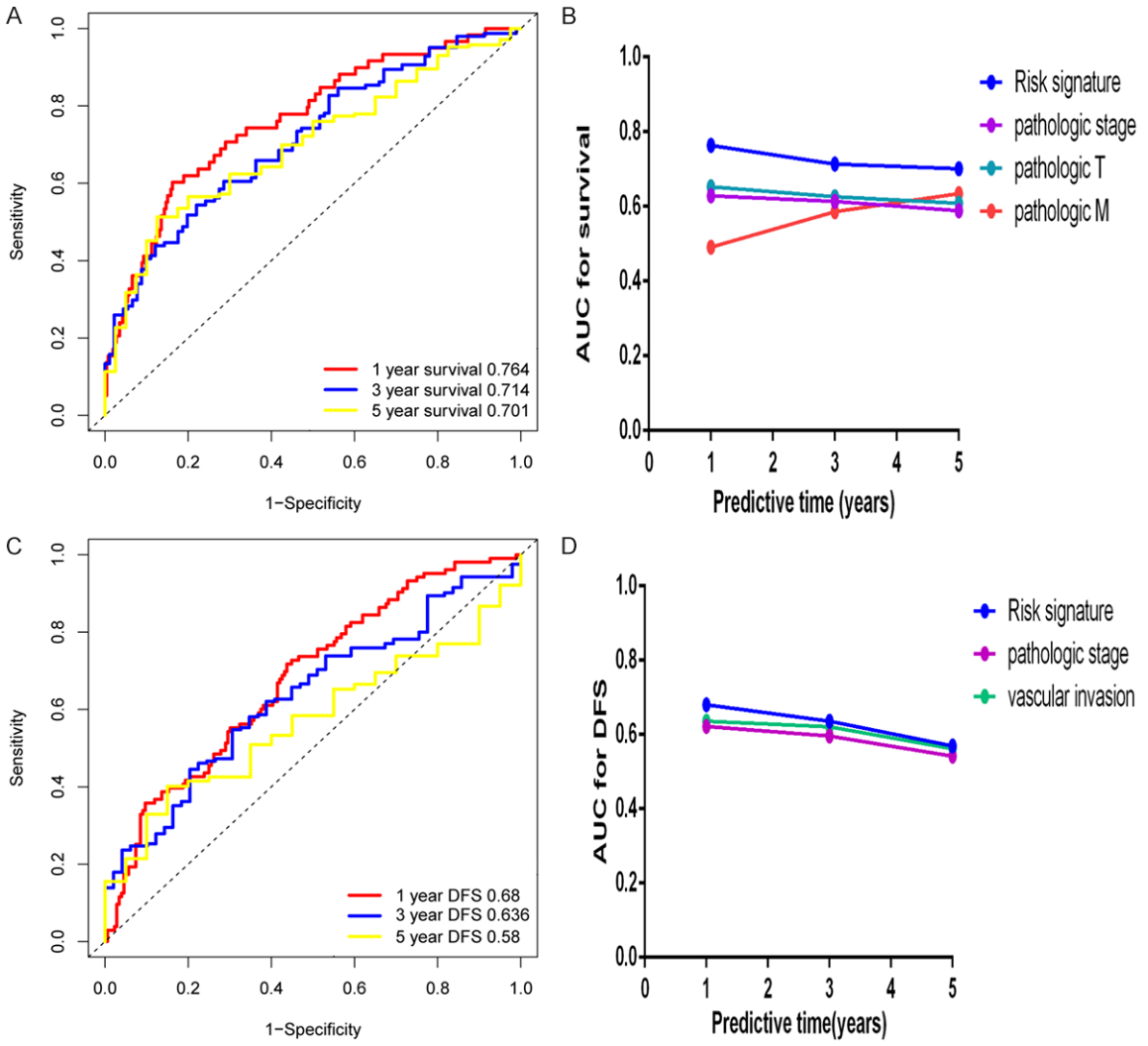


**Figure 5.** Predictive value of risk signature for OS and DFS of HCC patients in TCGA HCC cohort. A, C. The AUC of the risk signature for predicting 1-, 3- and 5-year OS and DFS were 0.76, 0.71, 0.70, 0.68, 0.64 and 0.58, respectively. B. Comparison of risk signature with pathologic stage, pathologic T stage and pathologic M stage in predicting 1-, 3- and 5-year OS of HCC patients, and the risk signature showed better predictive efficiency than others; D. Comparison of risk signature with pathologic stage and vascular invasion in predicting 1-, 3- and 5-year DFS of HCC patients, and the risk signature also showed better predictive efficiency than others.

genes in HCC patients is rarely systematically analyzed.

In the present study, we identified key hypoxia associated genes that were differentially expressed and relevant for prognosis predictions and therapeutic targets in HCC patients by analyzing high-throughput RNA-seq data downloaded from TCGA database. A total of 68 out of 84 genes were differentially expressed in HCC patients, which included 51 upregulated and 17 downregulated genes. Then, we identified two clusters of HCC patients with distinct clinical parameters and prognosis by applying consensus clustering of hypoxia associated genes. Next, 10 genes associated with OS were identified and a risk signature developed with these genes was found to effectively stratify patients into two distinct subgroups with different OS and DFS. The risk signature also showed better predictive efficiency than TNM stage in predicting the OS and DFS. In addition, we also tried to explore the potential mechanism by which Cluster status and the risk signature influenced prognosis and the landscape of tumor-infiltrating immune cells in patients with different

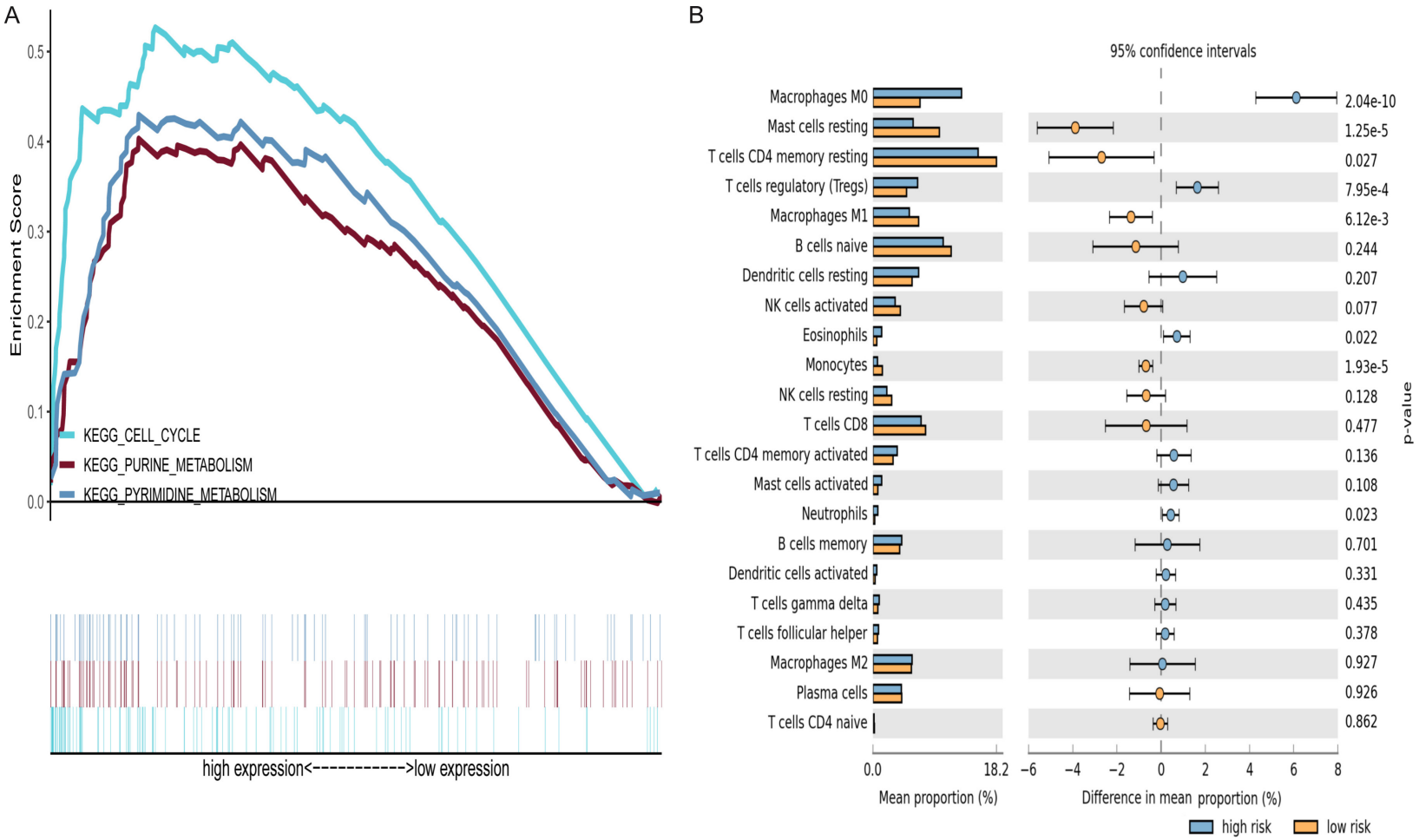


**Figure 6.** Potential mechanism by which the risk signature influenced prognosis and the landscape of tumor-infiltrating immune cells in patients with risk score. A. Gene set enrichment analysis of in patients with risk score in the TCGA HCC cohort, and KEGG pathways, “Cell cycle”, “Pyrimidine metabolism” and “Purine metabolism” were significantly enriched in patients with high risk score; B. Landscape of tumor-infiltrating immune cells in patients with different risk score in the TCGA HCC cohort, and patients with high risk score exhibited an immune-inhibited phenotype.

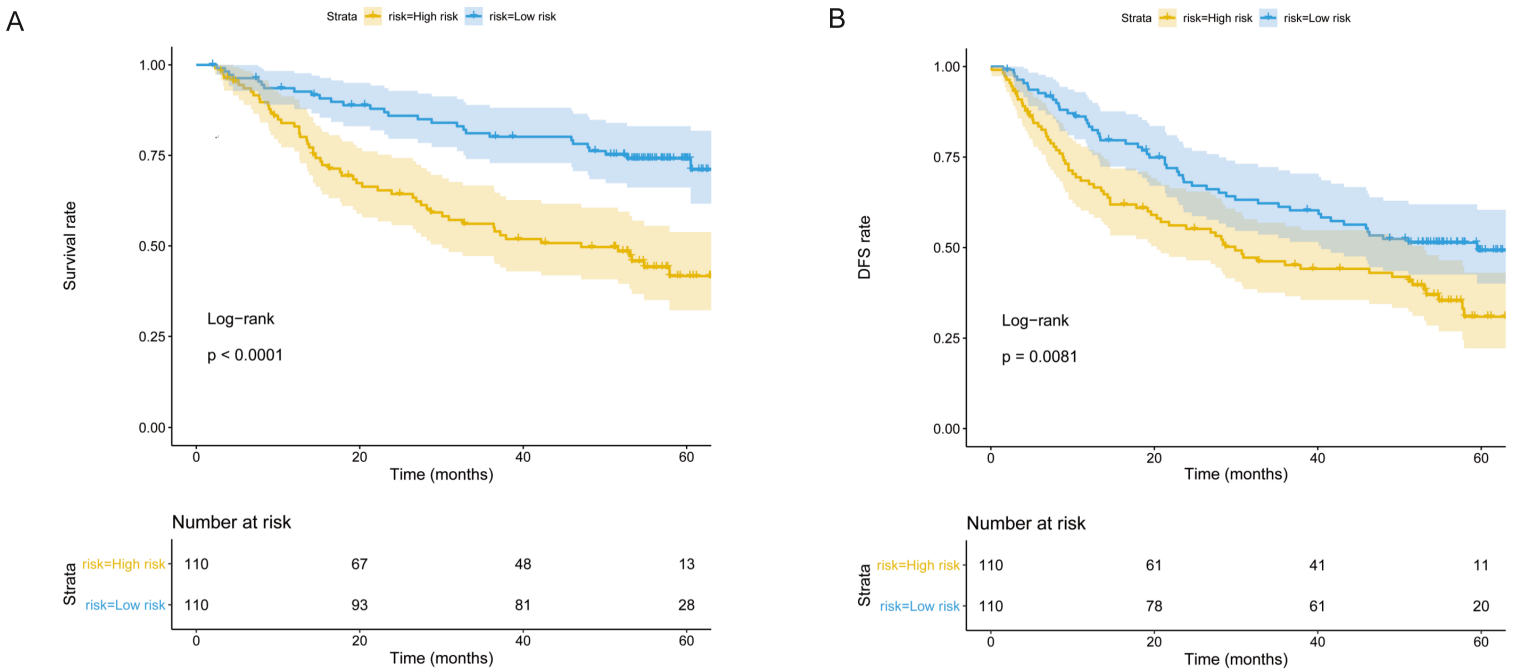
A
Strata risk=High risk risk=Low risk
Survival rate
1.00
0.75
0.50
0.25
0.00
Log−rank
p < 0.0001
0
20
40
60
Time (months)
Number at risk
Strata
risk=High risk 110 67 48 13
risk=Low risk 110 93 81 28
0
20
40
60
Time (months)
B
Strata risk=High risk risk=Low risk
DFS rate
1.00
0.75
0.50
0.25
0.00
Log−rank
p = 0.0081
0
20
40
60
Time (months)
Number at risk
Strata
risk=High risk 110 61 41 11
risk=Low risk 110 78 61 20
0
20
40
60
Time (months)

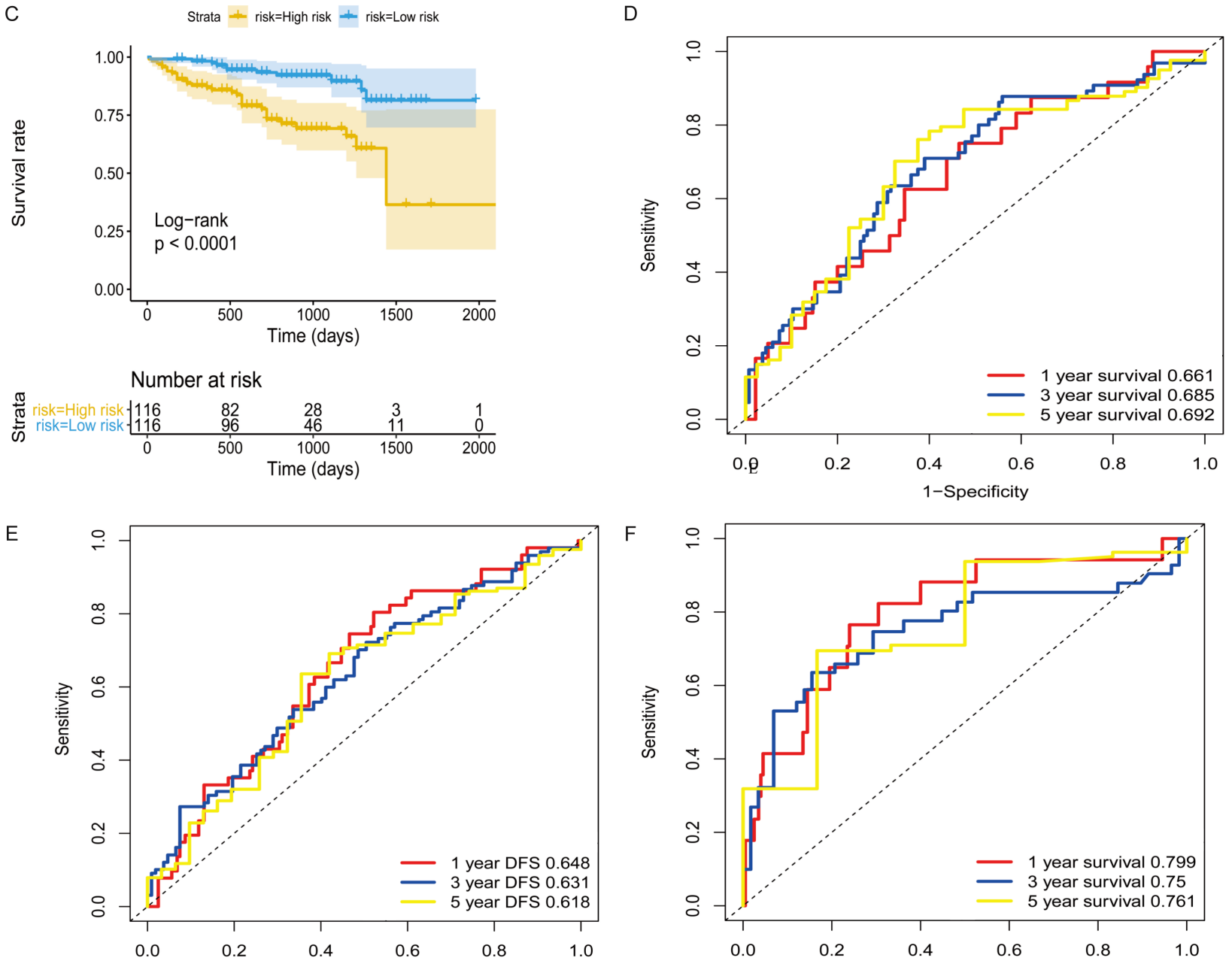
C
Strata
risk=High risk
risk=Low risk
Survival rate
1.00
0.75
0.50
0.25
0.00
Log−rank
p < 0.0001
0
500
1000
1500
2000
Time (days)
Number at risk
Strata
risk=High risk
risk=Low risk
116
82
28
3
1
116
96
46
11
0
0
500
1000
1500
2000
Time (days)
D
Sensitivity
1−Specificity
0.0
0.2
0.4
0.6
0.8
1.0
1 year survival 0.661
3 year survival 0.685
5 year survival 0.692
E
Sensitivity
1 year DFS 0.648
3 year DFS 0.631
5 year DFS 0.618
F
Sensitivity
1 year survival 0.799
3 year survival 0.75
5 year survival 0.761

**Figure 7.** Validation of risk signature in GSE14520 cohort and LIRI-JP cohort. A, B. Kaplan-Meier analysis for OS and DFS of patients with different risk scores in the GSE14520 cohort, and patients in the high risk subgroup had poorer OS and shorter DFS. C. Kaplan-Meier analysis of OS of patients with different risk scores in the LIRI-JP cohort, and patients in the high risk subgroup had poorer OS. D, E. The AUC of the risk signature for predicting 1-, 3- and 5-year OS and DFS of HCC patients from GSE14520 cohort were 0.66, 0.68, 0.69, 0.65, 0.63 and 0.62, respectively. F. The AUC of the risk signature for predicting 1-, 3- and 5-year OS were 0.80, 0.75 and 0.76, respectively.

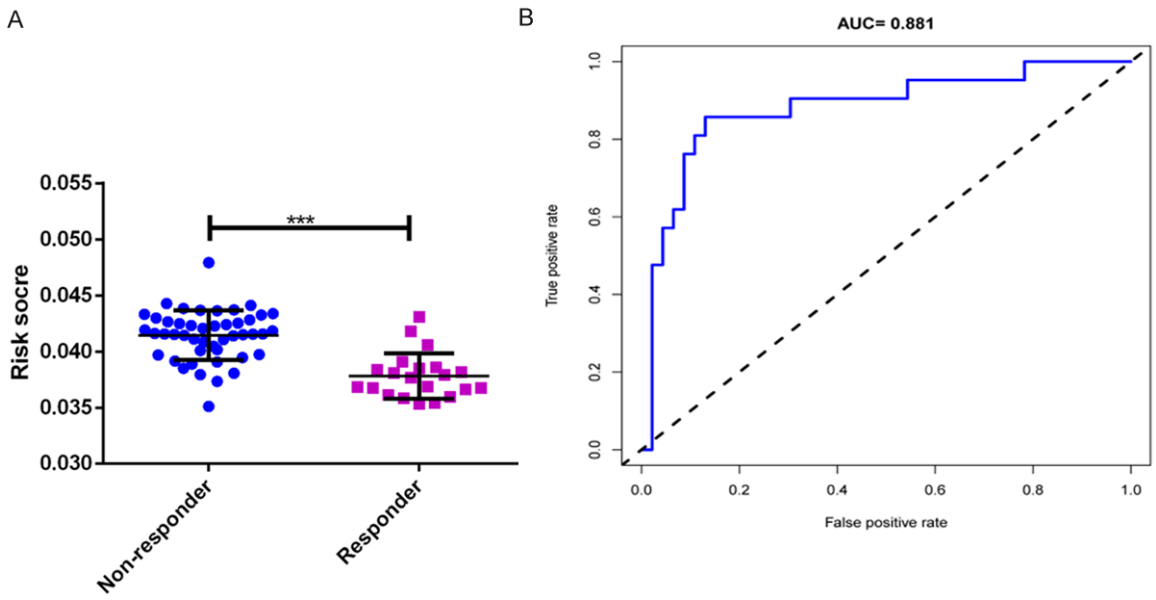


**Figure 8.** Relationship of risk signature with sorafenib treatment response. A. Difference of risk score between sorafenib treatment responders and nonresponders, and significantly higher risk scores were found at sorafenib treatment non-responders. B. The AUC of risk signature in predicting sorafenib treatment response was 0.881.

Cluster status or risk score. Furthermore, the good discrimination and prognostic value of the risk signature was also validated in the GSE14520 cohort and LIRI-JP cohort. Finally, the prediction values of the risk signature in sorafenib treatment response were also evaluated in the GSE109211 cohort.

Previously, 3 TCGA HCC clusters were identified by the TCGA Research Network by integrating multiple genomic data types. Unfortunately, no significant difference in OS was found among these three TCGA HCC clusters; the reason may possibly be due to the relatively short follow-up times in this dataset, with a median follow-up of 18 months [23]. However, as was also pointed out by Bévant K et al. on the common for the study by the TCGA Research Network, the absence of significant differences in term of survival between these 3 TCGA HCC clusters may challenge the validity of integrating all genomic data types simultaneously for cluster. Bévant K et al. thought that it would be interesting to explore whether some specific data types (such as quantitative mRNA levels) were more efficient than others in patient stratification [24]. In line with the view of Bévant K et al., in our study, we identified two clusters of HCC patients with distinct clinical parameters and prognosis by applying consensus clustering of 84 hypoxia associated genes. There were significantly more patients with advanced histologic grade, pathologic T stage and pathologic stage or patients with positive margin status and vascular invasion in Cluster 2. Consistent with these findings, patients in Cluster 2 had shorter OS and DFS compared to patients in Cluster 1. The Cluster status was significantly related to OS and DFS and it was also an independent prognostic factor for OS and DFS of HCC patients, suggesting that expression of these 84 hypoxia associated genes may be used to stratify HCC patients.

In addition, we explored the potential mechanism by which Cluster status influenced prog-

nosis. Based on the GSEA between Cluster 2 and Cluster 1, KEGG pathways, such as "Cell cycle", "Pathways in cancer", "P53 signaling pathway", "TGF-β signaling pathway", "WNT signaling pathway" and "MAPK signaling pathway" were significantly enriched in patients of Cluster 2 compared to that of Cluster 1. All aforementioned biological processes have been found to be involved in the formation of HCC [25-29], which may provide straight evidence for the rationality and molecular hypothesis of Cluster status in the stratification of HCC patients. Moreover, we also further analyzed the landscape of tumor-infiltrating immune cells in patients with different Cluster status and found that macrophage M0 cells, activated CD4 memory cells, neutrophils, plasma cells and memory B cells were enriched in patients of Cluster 2. Previous studies have shown that macrophages/monocytes could be recruited to the hypoxic regions of tumor tissues and became pro-angiogenic cells by upregulation of TIE2 expression, as these TIE2-positive macrophages/monocytes were correlated significantly with microvessel density in HCC. Increased TIE2-positive macrophages/monocytes were significantly associated with poorer OS and DFS and was also an independent prognostic factor for HCC patients [30, 31]. Zhou et al. also showed that tumor-associated neutrophils could recruit macrophages and T regulatory cells to promote the progression of HCC and resistance to sorafenib [32]. In addition, patients in Cluster 1 seemed to have higher immune infiltration of T and B cells, and the degree of tumor-infiltrating T and B cells correlated with the improved survival of HCC patients [33]. Taken, together, different kinds of tumor-infiltrating immune cells in patients with distinct Cluster status may contribute to their different prognosis. However, the potential mechanisms by which Cluster status contributed to hepato-carcinogenesis still remains largely understood, and further exploration of underlyin mechanisms are still necessary.

Next, a hypoxia associated genes based prognostic signature was developed with expression of 10 genes by univariate Cox regression and LASSO regression analyses using TCGA cohort. With the risk signature, HCC patients could be effectively stratified into two distinct subgroups with different OS and DFS. Besides, the risk signature was an independent prognostic factor for OS and DFS when adjusted for other clinical characteristics. The risk signature also showed better predictive power than pathologic TNM stage, which is commonly recommended as a prognostic factor in predicting OS and DFS (especially in predicting OS). The robustness of the risk signature was also validated in the GSE14520 cohort and LIRI-JP cohort. With the help of the risk signature, more intensive follow-up and even active adjuvant treatment may be needed for high risk HCC patients to reduce their relapse and improve their prognosis. On the other hand, less active follow-up may be needed for HCC patients with low risk, and they may even avoid the unbearable adverse effects of adjuvant therapies. In addition, we also found that significantly lower risk scores were found in sorafenib treatment responders compared to nonresponders, and the AUC for predicting sorafenib treatment response was 0.881, indicating that the risk signature may also be used as indicator for prediction of sorafenib treatment response and be used to identify HCC patients suitable for sorafenib treatment (as only approximately 30% of patients can benefit from sorafenib treatment) [34]. Consequently, the risk signature may be useful in setting up personalized surveillance schedules and selection of treatment strategies for HCC patients.

The 10 genes used for developing the prognostic signature corresponded to APEX1, ATR, CTSA, DNAJC5, ENO1, EPO, HMOX1, LDHA, NDRG1 and PER1. Of these, APEX1, ENO1, EPO, HMOX1, LDHA, NDRG1 and PER1 have been found to be related to HCC [35-41]. For example, Zhu et al. found that ENO1 was upregulated in HCC and related with worse OS and DFS. ENO1 expression was also independently associated with factor prognosis of HCC and may serve as a biomarker for diagnosis [36]. Yang et al. showed that EPO expression was correlated with vasculogenic mimicry formation. HCC patients with higher EPO expression exhibited poorer OS than patients with lower EPO expression. EPO expression was also an independent factor for prognosis of HCC [37]. Mechanistically, we also explored the biological process of the risk signature. Our results showed that the KEGG pathways of "Cell cycle", "Pyrimidine metabolism", and "Purine metabolism" were significantly enriched in patients from the high risk group. In agreement with our findings, Yeh et al. reported that an aberrant pyrimidine pathway found in patients with poor-

ly differentiated HCC could promote cancer stemness and serve as a potential therapeutic target for treatment of HCC tumor progression [42]. Moreover, macrophage M0 cells, regulatory T cells and neutrophils were enriched in patients from the high-risk group, which was similar to patients in Cluster 2, indicating that the risk signature may exploit a mechanism similar to Cluster status to influence the prognosis of patients with a high risk score.

Although the risk signature showed good performance in its discrimination and predictive ability for HCC patients, it still has some limitations. Firstly, the risk signature was developed on the basis of retrospective study data. Future prospective studies and validation are still needed with a larger sample size. Second, we did not directly analyze the potential mechanism of risk signature in HCC development and progression. In vitro studies are also needed to validate the potential mechanisms uncovered by bioinformatics. Finally, noninvasive 'liquid biopsy' is increasingly considered to have revolutionized in the field of cancer treatment and diagnosis [43]. The presence of these 10 genes in the blood samples or the predicting value of signature is worthy of exploration.

## Conclusion

Overall, we developed and validated a risk signature with the expression of 10 hypoxia associated ted genes, which reinforce the prediction of both prognosis and sorafenib treatment response in HCC patients.

## Acknowledgements

This study was supported by China Postdoctoral Science Foundation (No. 2020M682626) and Wu Jieping Medical Foundation (No. 320.6750.17528).

## Disclosure of conflict of interest

None.

## Abbreviations

HIF-1, hypoxia induced factor-1; TCGA, The Cancer Genome Atlas; ICGC, International Cancer Genome Consortium; GEO, gene expression omnibus; LASSO, least absolute shrinkage and selection operator; OS, overall survival; DFS, disease free status; LASSO, least absolute shrinkage and selection operator; GSEA, gene set enrichment analysis; AUC, areas under ROC curve.

**Address correspondence to:** Wei-Biao Lv, Department of Clinical Laboratory, Shunde Hospital, Southern Medical University (The First People's Hospital of Shunde), Foshan 528308, Guangdong Province, PR China. E-mail: weibiao2004@163.com

## References

[1] Bray F, Ferlay J, Soerjomataram I, Siegel RL, Torre LA and Jemal A. Global cancer statistics 2018: GLOBOCAN estimates of incidence and mortality worldwide for 36 cancers in 185 countries. CA Cancer J Clin 2018; 68: 394-424.

[2] Torre LA, Bray F, Siegel RL, Ferlay J, Lortet-Tieulent J and Jemal A. Global cancer statistics, 2012. CA Cancer J Clin 2015; 65: 87-108.

[3] El-Serag HB, Marrero JA, Rudolph L and Reddy KR. Diagnosis and treatment of hepatocellular carcinoma. Gastroenterology 2008; 134: 1752-1763.

[4] Yang JD, Hainaut P, Gores GJ, Amadou A, Plymoth A and Roberts LR. A global view of hepatocellular carcinoma: trends, risk, prevention and management. Nat Rev Gastroenterol Hepatol 2019; 16: 589-604.

[5] Tabrizian P, Jibara G, Shrager B, Schwartz M and Roayaie S. Recurrence of hepatocellular cancer after resection: patterns, treatments, and prognosis. Ann Surg 2015; 261: 947-955.

[6] McKeown SR. Defining normoxia, physoxia and hypoxia in tumours-implications for treatment response. Br J Radiol 2014; 87: 20130676.

[7] Chen C and Lou T. Hypoxia inducible factors in hepatocellular carcinoma. Oncotarget 2017; 8: 46691-46703.

[8] Piret JP, Minet E, Cosse JP, Ninane N, Debacq C, Raes M and Michiels C. Hypoxia-inducible factor-1-dependent overexpression of myeloid cell factor-1 protects hypoxic cells against tert-butyl hydroperoxide-induced apoptosis. J Biol Chem 2005; 280: 9336-9344.

[9] von Marschall Z, Cramer T, Hocker M, Finkenzeller G, Wiedenmann B and Rosewicz S. Dual mechanism of vascular endothelial growth factor upregulation by hypoxia in human hepatocellular carcinoma. Gut 2001; 48: 87-96.

[10] Gwak GY, Yoon JH, Kim KM, Lee HS, Chung JW and Gores GJ. Hypoxia stimulates proliferation of human hepatoma cells through the induction of hexokinase II expression. J Hepatol 2005; 42: 358-364.

[11] Zhou J, Schmid T, Schnitzer S and Brune B. Tumor hypoxia and cancer progression. Cancer Lett 2006; 237: 10-21.

[12] Kim YB, Park YN and Park C. Increased proliferation activities of vascular endothelial cells

and tumour cells in residual hepatocellular carcinoma following transcatheter arterial embolization. Histopathology 2001; 38: 160-166.
[13] Xiang Q, Dai X, Deng Y, He C, Wang J, Feng J and Dai Z. Missing value imputation for microarray gene expression data using histone acetylation information. BMC Bioinformatics 2008; 9: 252.
[14] Roessler S, Jia HL, Budhu A, Forgues M, Ye QH, Lee JS, Thorgeirsson SS, Sun Z, Tang ZY, Qin LX and Wang XW. A unique metastasis gene signature enables prediction of tumor relapse in early-stage hepatocellular carcinoma patients. Cancer Res 2010; 70: 10202-10212.
[15] Fujimoto A, Furuta M, Totoki Y, Tsunoda T, Kato M, Shiraishi Y, Tanaka H, Taniguchi H, Kawakami Y, Ueno M, Gotoh K, Ariizumi S, Wardell CP, Hayami S, Nakamura T, Aikata H, Arihiro K, Boroevich KA, Abe T, Nakano K, Maejima K, Sasaki-Oku A, Ohsawa A, Shibuya T, Nakamura H, Hama N, Hosoda F, Arai Y, Ohashi S, Urushidate T, Nagae G, Yamamoto S, Ueda H, Tatsuno K, Ojima H, Hiraoka N, Okusaka T, Kubo M, Marubashi S, Yamada T, Hirano S, Yamamoto M, Ohdan H, Shimada K, Ishikawa O, Yamaue H, Chayama K, Miyano S, Aburatani H, Shibata T and Nakagawa H. Whole-genome mutational landscape and characterization of noncoding and structural mutations in liver cancer. Nat Genet 2016; 48: 500-509.
[16] Gao J, Kwan PW and Shi D. Sparse kernel learning with LASSO and Bayesian inference algorithm. Neural Netw 2010; 23: 257-264.
[17] Subramanian A, Tamayo P, Mootha VK, Mukherjee S, Ebert BL, Gillette MA, Paulovich A, Pomeroy SL, Golub TR, Lander ES and Mesirov JP. Gene set enrichment analysis: a knowledge-based approach for interpreting genome-wide expression profiles. Proc Natl Acad Sci U S A 2005; 102: 15545-15550.
[18] Newman AM, Liu CL, Green MR, Gentles AJ, Feng W, Xu Y, Hoang CD, Diehn M and Alizadeh AA. Robust enumeration of cell subsets from tissue expression profiles. Nat Methods 2015; 12: 453-457.
[19] Parks DH, Tyson GW, Hugenholtz P and Beiko RG. STAMP: statistical analysis of taxonomic and functional profiles. Bioinformatics 2014; 30: 3123-3124.
[20] Yang SL, Liu LP, Jiang JX, Xiong ZF, He QJ and Wu C. The correlation of expression levels of HIF-1alpha and HIF-2alpha in hepatocellular carcinoma with capsular invasion, portal vein tumor thrombi and patients' clinical outcome. Jpn J Clin Oncol 2014; 44: 159-167.
[21] Mao CS, Yin H, Ning HB, Peng Z, Li K and Ding GQ. Levels of HBx, VEGF, and CEACAM1 in HBV-related hepatocellular carcinoma and their correlation with cancer prognosis. Eur Rev Med Pharmacol Sci 2017; 21: 3827-3833.
[22] Li W, Liang Y, Yang B, Sun H and Wu W. Downregulation of ARNT2 promotes tumor growth and predicts poor prognosis in human hepatocellular carcinoma. J Gastroenterol Hepatol 2015; 30: 1085-1093.
[23] Comprehensive and integrative genomic characterization of hepatocellular carcinoma. Cell 2017; 169: 1327-1341, e23.
[24] Bevant K and Coulouarn C. Landscape of genomic alterations in hepatocellular carcinoma: current knowledge and perspectives for targeted therapies. Hepatobiliary Surg Nutr 2017; 6: 404-407.
[25] Gong Z, Chi C, Huang X, Chu H, Wang J, Du F, Jiang L and Chen J. Cyclophilin A is overexpressed in hepatocellular carcinoma and is associated with the cell cycle. Anticancer Res 2017; 37: 4443-4447.
[26] Meng X, Franklin DA, Dong J and Zhang Y. MDM2-p53 pathway in hepatocellular carcinoma. Cancer Res 2014; 74: 7161-7167.
[27] Chen J, Gingold JA and Su X. Immunomodulatory TGF-beta signaling in hepatocellular carcinoma. Trends Mol Med 2019; 25: 1010-1023.
[28] Wang W, Smits R, Hao H and He C. Wnt/beta-catenin signaling in liver cancers. Cancers (Basel) 2019; 11: 926-946.
[29] Delire B and Starkel P. The Ras/MAPK pathway and hepatocarcinoma: pathogenesis and therapeutic implications. Eur J Clin Invest 2015; 45: 609-623.
[30] Matsubara T, Kanto T, Kuroda S, Yoshio S, Higashitani K, Kakita N, Miyazaki M, Sakakibara M, Hiramatsu N, Kasahara A, Tomimaru Y, Tomokuni A, Nagano H, Hayashi N and Takehara T. TIE2-expressing monocytes as a diagnostic marker for hepatocellular carcinoma correlates with angiogenesis. Hepatology 2013; 57: 1416-1425.
[31] He YF, Wang CQ, Yu Y, Qian J, Song K, Sun QM and Zhou J. Tie2-expressing monocytes are associated with identification and prognoses of hepatitis B virus related hepatocellular carcinoma after resection. PLoS One 2015; 10: e0143657.
[32] Zhou SL, Zhou ZJ, Hu ZQ, Huang XW, Wang Z, Chen EB, Fan J, Cao Y, Dai Z and Zhou J. Tumor-associated neutrophils recruit macrophages and t-regulatory cells to promote progression of hepatocellular carcinoma and resistance to sorafenib. Gastroenterology 2016; 150: 1646-1658, e17.
[33] Garnelo M, Tan A, Her Z, Yeong J, Lim CJ, Chen J, Lim KH, Weber A, Chow P, Chung A, Ooi LL, Toh HC, Heikenwalder M, Ng IO, Nardin A, Chen Q, Abastado JP and Chew V. Interaction between tumour-infiltrating B cells and T cells controls the progression of hepatocellular carcinoma. Gut 2017; 66: 342-351.

[34] Sanoff HK, Chang Y, Lund JL, O'Neil BH and Dusetzina SB. Sorafenib effectiveness in advanced hepatocellular carcinoma. Oncologist 2016; 21: 1113-1120.
[35] Cheng TL, Chen PS, Li RH, Yuan SS, Su IJ and Hung JH. Induction of apurinic endonuclease 1 overexpression by endoplasmic reticulum stress in hepatoma cells. Int J Mol Sci 2014; 15: 12442-12457.
[36] Zhu W, Li H, Yu Y, Chen J, Chen X, Ren F, Ren Z and Cui G. Enolase-1 serves as a biomarker of diagnosis and prognosis in hepatocellular carcinoma patients. Cancer Manag Res 2018; 10: 5735-5745.
[37] Yang Z, Sun B, Zhao X, Shao B, An J, Gu Q, Wang Y, Dong X, Zhang Y and Qiu Z. Erythropoietin and erythropoietin receptor in hepatocellular carcinoma: correlation with vasculogenic mimicry and poor prognosis. Int J Clin Exp Pathol 2015; 8: 4033-4043.
[38] Yeh CN, Wu RC, Cheng CT, Tsai CY, Chang YR, Yeh TS, Wu TH, Lee WC and Chiang KC. HO-1 is a favorable prognostic factor for HBV-HCC patients who underwent hepatectomy. Cancer Manag Res 2018; 10: 6049-6059.
[39] Guo Y, Li X, Sun X, Wang J, Yang X, Zhou X, Liu X, Liu W, Yuan J, Yao L and Shen L. Combined aberrant expression of NDRG2 and LDHA predicts hepatocellular carcinoma prognosis and mediates the anti-tumor effect of gemcitabine. Int J Biol Sci 2019; 15: 1771-1786.
[40] Cheng J, Xie HY, Xu X, Wu J, Wei X, Su R, Zhang W, Lv Z, Zheng S and Zhou L. NDRG1 as a biomarker for metastasis, recurrence and of poor prognosis in hepatocellular carcinoma. Cancer Lett 2011; 310: 35-45.
[41] Zhang Z, Ma F, Zhou F, Chen Y, Wang X, Zhang H, Zhu Y, Bi J and Zhang Y. Functional polymorphisms of circadian negative feedback regulation genes are associated with clinical outcome in hepatocellular carcinoma patients receiving radical resection. Med Oncol 2014; 31: 179.
[42] Yeh HW, Lee SS, Chang CY, Hu CM and Jou YS. Pyrimidine metabolic rate limiting enzymes in poorly-differentiated hepatocellular carcinoma are signature genes of cancer stemness and associated with poor prognosis. Oncotarget 2017; 8: 77734-77751.
[43] Bettegowda C, Sausen M, Leary RJ, Kinde I, Wang Y, Agrawal N, Bartlett BR, Wang H, Luber B, Alani RM, Antonarakis ES, Azad NS, Bardelli A, Brem H, Cameron JL, Lee CC, Fecher LA, Gallia GL, Gibbs P, Le D, Giuntoli RL, Goggins M, Hogarty MD, Holdhoff M, Hong SM, Jiao Y, Juhl HH, Kim JJ, Siravegna G, Laheru DA, Lauricella C, Lim M, Lipson EJ, Marie SK, Netto GJ, Oliner KS, Olivi A, Olsson L, Riggins GJ, Sartore-Bianchi A, Schmidt K, Shih I M, Oba-Shinjo SM, Siena S, Theodorescu D, Tie J, Harkins TT, Veronese S, Wang TL, Weingart JD, Wolfgang CL, Wood LD, Xing D, Hruban RH, Wu J, Allen PJ, Schmidt CM, Choti MA, Velculescu VE, Kinzler KW, Vogelstein B, Papadopoulos N and Diaz LA Jr. Detection of circulating tumor DNA in early- and late-stage human malignancies. Sci Transl Med 2014; 6: 224ra224.

## Supplemental materials

*84 hypoxia signaling pathway related genes*

HIF1 & Co-Transcription Factors: ARNT, COPS5, HIF1A, HIF1AN, HIF3A, HNF4A, NCOA1, PER1.
Other HIF1 Interactors: APEX1, EGLN1, EGLN2, NFKB1, P4HA1, P4HB, TP53.

Responsive genes:
Angiogenesis: ADORA2B, ANGPTL4, ANXA2, BTG1, EGR1, EDN1, EPO, F3, GPI, HMOX1, JMJD6, LOX, MMP9, PGF, PLAU (uPA), SERPINE1 (PAI-1), VEGFA.
Coagulation: ALDOA, ANXA2, F10, F3, F3, PLAU (uPA), SERPINE1 (PAI-1), SLC16A3.
DNA Damage Signaling & Repair: ATR, MIF, NDRG1, RUVBL2.
Metabolism: ALDOA, DDIT4 (REDD1), ENO1, ERO1L, GBE1, GPI, GYS1, HK2, LDHA, PDK1, PFKFB3, PFKFB4, PFKL, PFKP, PGAM1, PGK1, PKM2, SLC2A1, SLC2A3, TPI1.
Regulation of Apoptosis: ADM, BNIP3, BNIP3L, BTG1, DDIT4 (REDD1), IER3, MIF, NOS3 (eNOS), PIM1.
Regulation of Cell Proliferation: ADM, BTG1, BLM, CCNG2, EGR1, IGFBP3, MET, MIF, MXI1, NAMPT, NOS3 (eNOS), ODC1, PGF, PIM1, TXNIP.
Transcription Factors: BHLHE40, FOS, RBPJ, USF2.
Transporters, Channels & Receptors: SLC2A1, SLC2A3, SLC16A3, TFRC, VDAC1.
Other Responsive Genes: ANKRD37, CA9, CTSA, DNAJC5, EIF4EBP1, LGALS3, MAP3KI.